PCCP

Effect of molecular structure and hydrogen bonding on the fluorescence of hydroxy-substituted naphthalimides

László Biczók,*[a] Pierre Valat[b] and Véronique Wintgens[b]

[a] *Chemical Research Center, Hungarian Academy of Sciences, P.O. Box 17, 1525 Budapest, Hungary*
[b] *Laboratoire des Matériaux Moléculaires, C.N.R.S., E.R. 241, 2, 8 rue H. Dunant, 94320 Thiais, France*

Received 7th June 1999, Accepted 23rd August 1999

Fluorescence properties of hydroxy-naphthalimides were studied in methylene chloride in the absence and the presence of hydrogen-bonding additives. The position of the HO-substituent only slightly affects the radiative rate, however, the triplet yield and the rate of the radiationless processes are considerably higher for the 3-hydroxy derivative. Addition of nitrogen-heterocyclic compounds leads not only to hydrogen-bonding in the ground state but also fluorescence quenching. The parallel change throughout the series of the hydrogen-bond acceptors between the proton affinity and the rate constants of dynamic quenching indicates that proton displacement plays a crucial role in the excited hydrogen-bonded complexes. Interaction of hydroxy-naphthalimides with pyridine and benzoxazole results in rapid radiationless deactivation from the singlet excited state, whereas intense emission as well as long fluorescence lifetime characterize imidazole and pyrazole complexes. The dual emission of the imidazole complexes observed in solvents of medium polarity is assigned to two conformers which differ in the extent of the proton shift along the hydrogen-bond.

Introduction

The molecular mechanism of the excited state relaxation induced by intermolecular hydrogen-bond formation is of great interest because it belongs to the most fundamental processes of photochemistry. Most of the studies in this field have dealt with the effect of the hydrogen-bond donors on the fluorescent properties of aromatic heterocyclic[1] and carbonyl compounds.[2–6] These molecules form hydrogen-bonded complexes with alcohols and hydroperoxides in the excited state and the hydrogen-bond acts as an efficient vibronic dissipative mode in the nonradiative transition.[2–6] On the other hand, coupled electron–proton movement was found to play a dominant role in the deactivation of excited hydrogen-bonded porphyrins[7,8] and Ru(II)polypyridyl complexes[8] as well as in the interaction of excited ketones with phenols.[4,9]

Picosecond laser photolysis studies established that excited hydrogen-bond donors, such as aromatic >N–H or –O–H compounds, are efficiently quenched by pyridine derivatives *via* non-fluorescent hydrogen-bonded complex, in which associated electron and proton displacement facilitates the charge transfer interaction between the two conjugate π-electronic systems.[10] However, when phenols form hydrogen-bonded complexes with aliphatic amines no charge delocalization is possible along the hydrogen-bond and photoexcitation induces proton transfer.[11]

The present paper focuses on the question of how the variation of the molecular structure of the hydrogen-bonding additive influences the fluorescent properties and the deactivation mechanism of the excited molecules. In order to reveal the role of aromaticity and proton affinity in the hydrogen-bonding induced quenching process, aromatic heterocyclic compounds were used as hydrogen-bond acceptors. We show examples where the excited hydrogen-bonded complexes emit dual fluorescence, which is assigned to two conformers differing in the extent of the proton shift along the hydrogen-bond. Hydroxy-substituted naphthalimides were chosen as model compounds in these studies because they have both hydrogen-bond donor and acceptor moieties, and, on the basis of our previous studies,[12] they are expected to be strongly fluorescent. In addition, the electron withdrawing character of the imide group probably enhances the acidity in the excited state and light absorption may serve as an ultrafast trigger for the proton transfer reaction. Recent studies of related compounds demonstrated that substitution of naphthols with cyano or methanesulfonyl groups markedly increases the photoacidity.[13–15]

Another main goal of this work was to examine how the introduction of a hydroxy substituent into the 1,8-naphthalimide moiety alters the dominant energy dissipating pathways occurring from the singlet excited state. The investigated compounds are given in Scheme 1.

Experimental

Acetonitrile, methylene chloride (Prolabo, HPLC grade), dimethylsulfoxide (Merck, spectroscopic grade) and trifluoroethanol (Aldrich) were used as received. Benzoxazole, imidazole, isoxazole, pyrazole and pyridine were purchased from Aldrich (highest quality available).

N-Methyl-1,8-naphthalimide (NI), also called 2-methyl-1*H*-benz[*d*,*e*]isoquinoline-1,3(2H)-dione, was available from our previous study.[16] 4-Hydroxy-*N*-methyl-1,8-naphthalimide (4-HONI), also called 6-hydroxy-2-methyl-1*H*-benz[*d*,*e*]

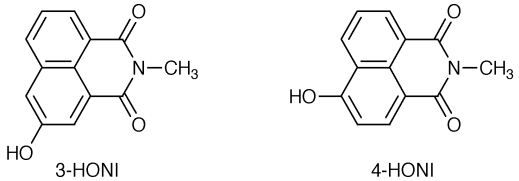

Scheme 1

isoquinoline-1,3(2H)-dione, was prepared by demethylation of 4-methoxy-*N*-methyl-1,8-naphthalimide,[17] following a procedure similar to one described previously.[18] One equivalent of the methoxy derivative mixed with 40 equivalents of pyridine hydrochloride was heated at 190 °C under argon for 35 min. After cooling, the solid reaction mixture was added to an aqueous HCl solution (1 M). The solid was filtered, washed with aqueous HCl solution (1 M) and water. The crude product was purified by dissolution in an aqueous Na_2CO_3 solution, followed by extraction with ether and precipitation by the addition of perchloric acid in the aqueous phase (45% yield), m.p. 298–302 °C (lit.[18] 303–305 °C).

3-Hydroxy-*N*-methyl-1,8-naphthalimide (3-HONI), also called 5-hydroxy-2-methyl-1*H*-benz[*d*,*e*]isoquinoline-1,3(2H)-dione, was synthesized *via* four reaction steps. First, 3-nitro-*N*-methyl-1,8-naphthalimide was prepared by condensation of 3-nitro-1,8-naphthalic anhydride (Aldrich) with methylamine hydrochloride in acetic acid. Then 1 equivalent of 3-nitro-*N*-methyl-1,8-naphthalimide was reduced by 4 equivalents of tin(II)chloride in hot hydrochloric acid.[19] The obtained amino derivative was diazotized and the diazonium salt was hydrolyzed by aqueous HCl solution. The final product was purified by the method described for 4-HONI (15% yield, m.p. 249–251 °C).

The UV–visible absorption spectra were obtained with a Varian–Cary model 50 Bio apparatus. Fluorescence spectra were recorded with an SLM-Aminco model 8100 device. Fluorescence quantum yields of 3-HONI and 4-HONI were determined by comparison with that of 4-methoxy-*N*-methyl-1,8-naphthalimide in acetonitrile solution, for which a reference yield of $\Phi_F = 0.88$ was taken.[12] Singlet lifetimes were measured by excitation with a B.M. Industries frequency-tripled Nd–YAG laser (pulse duration 30 ps FWHM), using the experimental set-up already described.[20] Laser flash photolysis experiments were carried out with 8 ns FWHM pulse of a Nd–YAG laser and the monitoring light from Applied Photophysics xenon lamp passed through the sample perpendicular to the excitation. Intersystem crossing (ISC) quantum yields were determined in oxygen-free solutions relative to triplet benzophenone. We compared the initial triplet–triplet absorbances of the investigated compound (A) at 480 nm with that of the benzophenone reference (A_{ref}) at 530 nm. The solutions had matched absorbances at the excitation wavelength (355 nm). The triplet yields (Φ_{ISC}) were obtained based on the equation

$$\Phi_{ISC} = {}^3\Phi_{ref}(A/A_{ref})(\varepsilon_{ref}/\varepsilon) \quad (1)$$

using the well-established yield (${}^3\Phi_{ref} = 1.00$)[21] and molar absorption coefficient ($\varepsilon_{ref} = 7200\ M^{-1}\ cm^{-1}$ at 530 nm)[22] for triplet benzophenone, whereas $\varepsilon = 10\,000\ M^{-1}\ cm^{-1}$ was taken for the triplet molar absorption coefficient of naphthalimides at 480 nm.[16]

Results and discussion

I. Photophysical properties of hydroxy-naphthalimides

Absorption and fluorescence spectra. Fig. 1 presents the absorption and fluorescence spectra of hydroxy-naphthalimides in methylene chloride. The absorption spectra resemble those of the corresponding naphthols, however, the introduction of the imide moiety results in a remarkable bathochromic shift of the maxima, which becomes most apparent for the low energy bands. For the energy of the lowest excited singlet states, 308 kJ mol^{-1} and 300 kJ mol^{-1} were obtained from the locations of the intersections of the normalized absorption and fluorescence spectra in the case of 3-HONI and 4-HONI, respectively. The energy difference between the first absorption band of the hydroxy-naphthalimide and the corresponding naphthol was found to be more considerable for the 4-HO derivative. This clearly indicates the larger extent of conjugation between the electron donating OH and the electron withdrawing imide moiety in 4-HONI. The Stokes-shift of the fluorescence spectrum is more pronounced (78 nm) for 4-HONI compared with that of 3-HONI (35 nm). Changing the solvent from methylene chloride to acetonitrile leads to a 6 nm and 2 nm fluorescence maximum displacement for the former and the latter compounds, respectively. These small solvatochromic shifts together with the small decrease of the S_1 state energy with increasing solvent polarity (*vide infra*) suggest that the lowest excited singlet states have limited charge transfer character for both HONI isomers.

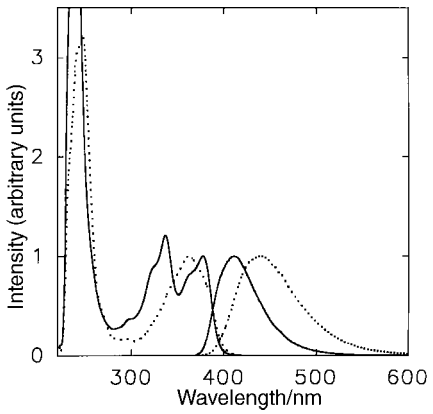

Fig. 1 Absorption and fluorescence spectra of 3-HONI (——) and 4-HONI (· · ·) in CH_2Cl_2.

Fig. 2 shows the excitation and the fluorescence spectra of the hydroxy-naphthalimides and their conjugated bases in acetonitrile. In this solvent we used 1.5×10^{-4} M perchloric acid to prevent the dissociation of the OH-moiety and to record solely the spectra corresponding to the phenolic form. In order to deprotonate the OH group, 2 μl of 1 M KOH in methanol was added into 2 ml of hydroxy-naphthalimide solution. Under these conditions, the spectra are assigned to the naphtholate anion and the bands are located at lower energies. Based on the intersection of the normalized excitation and fluorescence spectra, 305 kJ mol^{-1} and 210 kJ mol^{-1} were calculated for the energies of the first excited singlet state of 3-HONI and its conjugated base, respectively. A much

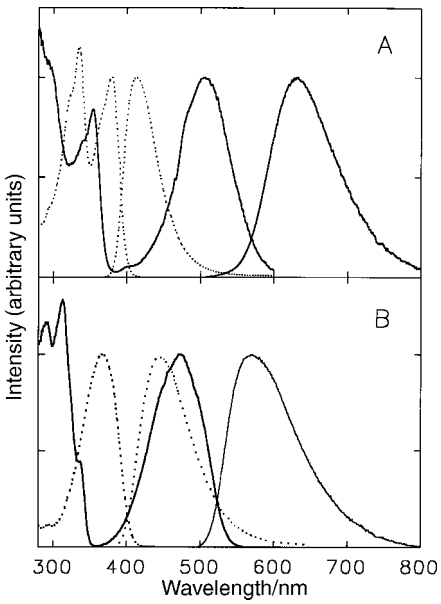

Fig. 2 Fluorescence and excitation spectra of (A) 3-HONI and (B) 4-HONI in acetonitrile. Phenolic form in the presence of 1.5×10^{-4} M perchloric acid (· · ·) and deprotonated anion form in the presence of 1×10^{-3} M KOH (——).

smaller difference was observed between the S_1 energies of 4-HONI and its deprotonated form (297 kJ mol^{-1} and 229 kJ mol^{-1}, respectively). According to the Förster cycle,[23] these results suggest that 4-HONI undergoes a smaller acidity enhancement upon electronic excitation. The lack of the long wavelength emission in CH_2Cl_2 clearly indicates that none of the singlet excited hydroxy-naphthalimides are sufficiently acidic to transfer proton to this solvent.

Photophysical properties. Table 1 demonstrates that substitution of *N*-methyl-1,8-naphthalimide (NI) with a hydroxy moiety leads to a considerable change in fluorescence yield (Φ_F), fluorescence lifetime (τ_F) and triplet yield (Φ_{ISC}). Fluorescence yields and lifetimes increase more than one order of magnitude through the series of NI, 3-HONI, 4-HONI, whereas the variation of the triplet yields exhibits the opposite tendency; they decrease parallel with the energy of the lowest excited singlet ($E(S_1)$). In order to get a deeper insight into the factors controlling the rate of the energy dissipating pathways, the rate constants for fluorescence (k_F), intersystem crossing (k_{ISC}) and internal conversion (k_{IC}) were derived using the expressions given below:

$$k_F = \Phi_F/\tau_F \quad (2)$$

$$k_{ISC} = \Phi_{ISC}/\tau_F \quad (3)$$

$$k_{IC} = (1 - \Phi_{ISC} - \Phi_F)/\tau_F \quad (4)$$

It is seen from the rate constants presented in Table 1 that fluorescence emission is the dominant process from the singlet excited state of 4-HONI, however, radiationless transitions prevail for 3-HONI. In contrast with the very fast intersystem crossing observed for unsubstituted NI,[16] triplet formation is fairly slow for both hydroxy-naphthalimides. This is especially true of the 4-HO derivative, where almost negligible k_{ISC} was found and the phosphorescence is extremely weak at 77 K in organic glass. In the case of 3-HONI the more efficient intersystem crossing permits the determination of the triplet–triplet absorption and the phosphorescence spectra. The triplet–triplet absorption maxima detected by a laser flash photolysis technique appear at 450 and 480 nm at ambient temperature in CH_2Cl_2, whereas the phosphorescence peaks can be found at 590 and 640 nm at 77 K in 95 : 5 butyronitrile: butyl acetate mixture. From the 0–0 transition of the phosphorescence the energy of the first triplet excited state is calculated to be 213 kJ mol^{-1}. This value is lower than the one found for *N*-methyl-1,8-naphthalimide (221 kJ mol^{-1}) indicating that substitution with an OH group not only decreases the energy of the S_1 state but also that of the T_1 state.

The efficient triplet formation for *N*-methyl-1,8-naphthalimide ($\Phi_{ISC} = 0.94$) was rationalized in terms of the transition from the lowest singlet excited state to a close-lying higher triplet state (T_n).[16] As we established in a previous paper,[16] this is a thermally enhanced process in moderately and strongly polar solvents, which results in a temperature dependent fluorescent behavior. However, the fluorescence lifetimes of 3-HONI and 4-HONI were found to be temperature independent in the 296–198 K range. Based on these results, we can exclude the thermally activated intersystem crossing pathway for hydroxy-naphthalimides. The electron donating hydroxy group decreases the S_1 state energy and thereby, increases the S_1–T_n energy gap. With such an increased energy gap, thermal activation is not able to initiate the endothermic $S_1 \rightarrow T_n$ transition, consequently, triplet formation can occur only by the slower transitions to lower triplet levels. Similar effects were observed for 4-methoxy-*N*-methyl-1,8-naphthalimide, which also has an electron donating moiety.[12]

The significant difference in the triplet formation rate constant between 3-HONI and 4-HONI (Table 1) can be rationalized based on the relative position of the singlet and the triplet energy levels. Semi-empirical calculation[24] showed that the S_1–T_1 energy gap is larger for 4-HONI compared with that of 3-HONI (144 kJ mol^{-1} and 132 kJ mol^{-1} were obtained, respectively). This larger energy gap may lessen the magnitude of the spin–orbit coupling between the S_1 and T_1 states leading to a slower intersystem crossing process for 4-HONI.

It is evident from the data summarized in Table 1 that the introduction of a hydroxy group into the 1,8-naphthalimide moiety in position 3 hardly influences the rate constant for internal conversion (k_{IC}), however, the $S_1 \rightarrow S_0$ radiationless transition is markedly decelerated for 4-HONI. It seems to be a general tendency that the 4-substitution of the 1,8-naphthalimide skeleton with an electron donating group leads to a reduced k_{IC}. This effect can be observed for HO–, CH_3O– and NH_2– derivatives alike. Prado *et al.* suggested[25] that the molecule has a quinoid resonance form if an electron donating group is attached to position 4. This kind of electron displacement, which can occur both in the S_1 and the S_0 states, may affect the vibronic coupling between these states and consequently, may lead to slower internal conversion.

II. Effect of hydrogen-bonding additives

In order to reveal how hydrogen-bonding influences the rate and the mechanism of the deactivation processes originating from the singlet excited state, we systematically varied the proton affinity, the hydrogen-bonding ability and the aromaticity of the additives using both hydrogen-bond donors and acceptors.

Trifluorethanol (TFE). We have previously shown that the fluorescence lifetime and quantum yield of *N*-methyl-1,8-naphthalimide considerably increase[16] in TFE, a solvent which has high hydrogen-bonding power. In the present work, we extend these studies to hydroxy-naphthalimides, In contrast with that found for the unsubstituted *N*-methyl-1,8-naphthalimide, addition of 0.035 M TFE does not influence the fluorescent behavior of its hydroxy-derivatives in CH_2Cl_2. A ten times higher amount of TFE caused a *ca.* 9 nm bathochromic shift of the fluorescence maxima for both the 3- and the 4-substituted derivatives, but neither fluorescence quenching nor appearance of a new emission band was observed. The excitation and ground state absorption spectra exhibited a red-shift as a function of the TFE concentration. The clear isosbestic points in the absorption spectra demonstrated that a 1 : 1 hydrogen-bonded complex formed with TFE. The equilibrium constants for hydrogen-bonding (K) were determined using the following relationship.[26]

$$[1 - (A_0/A)_\lambda]/[\text{additive}] = -K + K(\varepsilon_C/\varepsilon_A)_\lambda(A_0/A)_\lambda \quad (5)$$

where $(\varepsilon_C/\varepsilon_A)_\lambda$ is the ratio of the molar absorption coefficients for the complexed and free hydroxy-naphthalimides at a particular wavelength (λ), A_0 and A denotes the absorbances in

Table 1 Photophysical properties of hydroxy-naphthalimides in CH_2Cl_2

	λ_{abs}^{max}/nm	λ_F^{max}/nm	$E(S_1)$/kJ mol^{-1}	Φ_F	τ_F/ns	Φ_{ISC}	$k_F/10^7$ s^{-1}	$k_{IC}/10^7$ s^{-1}	$k_{ISC}/10^7$ s^{-1}
NI[a]	348	378	334	0.031	0.14	0.94[b]	22	21[b]	670[b]
3-HONI	376	411	308	0.13	1.9	0.50	6.8	19	26
4-HONI	362	440	300	0.85	9.0	0.03	9.4	1.3	0.3

[a] Ref. 16. [b] Based on triplet yield in acetonitrile.

the presence and the absence of TFE, respectively. Plotting the left-hand side of the function against $(A_0/A)_\lambda$ gives good linear correlation. From the intercepts, 1.5 M^{-1} and 1.1 M^{-1} hydrogen-bonding equilibrium constants were obtained for 3-HONI and 4-HONI, respectively. These values are comparable with that reported for fluorenone–TFE complex (0.7 M^{-1} in CH_2Cl_2)[4] where TFE is also attached to a carbonyl moiety.

Dimethylsulfoxide (DMSO). In contrast to the small effect of TFE hydrogen-bond acceptors, which interact with the HO-substituent, DMSO considerably alters the spectral behavior of hydroxy-naphthalimides. When weakly basic but strongly hydrogen-bonding DMSO is added to the hydroxy-naphthalimide solutions, characteristic changes are observed, which are demonstrated for 3-HONI in Fig. 3. The red-shift of the long-wavelength absorption band and the clear isosbestic points at 337, 346.5, 380 nm for the 3-hydroxy and at 366.5 nm for the 4-hydroxy derivatives indicate 1 : 1 hydrogen-bonded complex formation. From the effect of DMSO on the absorption spectra, the hydrogen-bonding equilibrium constants (K) were derived using eqn. (5). The average values of K calculated from the data measured at different wavelengths are 101 ± 15 M^{-1} and 191 ± 13 M^{-1} for the 3-HONI and 4-HONI complexes, respectively.

The fluorescence maximum gradually shifts to lower energies with increasing DMSO concentration and an isoemissive point appears but the quantum yield of fluorescence does not change significantly. As the red-shift is only *ca.* 11 nm, we assign the new fluorescence band to the hydrogen-bonded complex. This view is supported by the fact that DMSO does not bring about any significant change in the spectra of methoxy-naphthalimides, where no hydrogen-bonding is feasible. In addition, we can exclude proton transfer from the OH-group to DMSO because no fluorescence was detected in the 500–800 nm range, where emission from the conjugate base (anion) of the hydroxy-naphthalimides is expected (Fig. 2). The excitation and the absorption spectra showed similar changes indicating that hydrogen-bonding with DMSO in the ground state is the dominant process. The variation of the fluorescence intensity (I) as the function of [DMSO] was analyzed using a relationship analogous to eqn. (5).

$$[1 - (I_0/I)_F]/[\text{additive}] = -K + K(\varepsilon_C/\varepsilon_A)_\lambda(\Phi_C/\Phi_A)_F(I_0/I)_F \quad (6)$$

where $(I_0/I)_F$ represents the ratio of fluorescence intensities in the presence and the absence of DMSO, and $(\Phi_C/\Phi_A)_F$ is the ratio of fluorescence efficiencies for the complex and the free fluorophore at the detection wavelength.[26] Fitting this function to the experimental data leads to K values of 85 ± 9 M^{-1} and 195 ± 23 M^{-1} for the equilibrium constants for hydrogen-bonding of DMSO with 3-HONI and 4-HONI, respectively. The good agreement of these results with the corresponding values derived from absorption spectroscopic studies indicates that excitation of the complex does not cause significant change in the hydrogen-bonding equilibrium constant, *i.e.*, K is not significantly different for the excited and the ground state complex. Time-resolved fluorescence measurements proved that the dynamic quenching by DMSO is negligible. The lifetimes of the singlet excited hydrogen-bonded complexes of 3-HONI and 4-HONI are 2.2 ns and 9.3 ns, respectively. Since the lifetimes of the free and the complexed molecules agree very closely, we conclude that no energy dissipation takes place *via* the hydrogen-bond with DMSO.

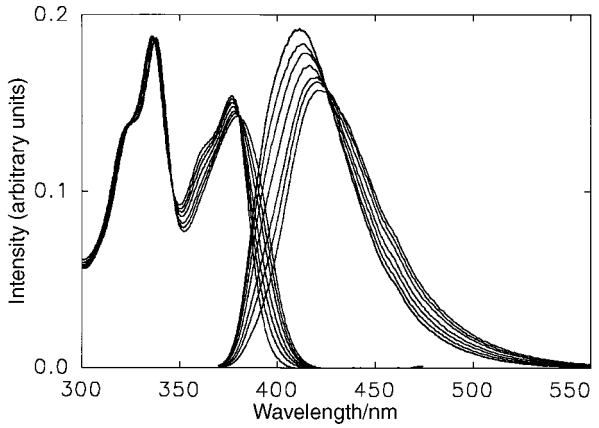

Fig. 3 Absorption and fluorescence spectra of 3-HONI in CH_2Cl_2 at different DMSO concentrations (0, 0.0014, 0.0035, 0.007, 0.014, 0.021, 0.035 M).

Pyridine. Addition of pyridine to the hydroxy-naphthalimide solutions in CH_2Cl_2 leads not only to hydrogen-bonding in the ground state but also to fluorescence quenching. The change in the absorption spectrum closely resembles that found in the case of DMSO. Plotting the absorbances according to eqn. (5), we determined the equilibrium constant of hydrogen-bonding (K). The average values of K derived from measurements at various wavelengths are summarized in Table 2.

The increase of the pyridine concentration in the 0–0.06 M range results in considerable fluorescence quenching but neither the appearance of a new band nor a shift of the maximum can be seen in the fluorescence spectra. Based on these observations, we conclude that the hydroxy-naphthalimide–pyridine hydrogen-bonded complexes have negligible fluorescence yield. The Stern–Volmer plot of the

Table 2 Hydrogen-bonding equilibrium constants and rate constants of fluorescence quenching

Quencher	Proton affinity/kJ mol^{-1}	Aromaticity index, I_x	K^a absorption/M^{-1}	K^b fluorescence/M^{-1}	k_q [c] lifetime/ 10^9 M^{-1} s^{-1}
3-Hydroxy-naphthalimide—					
Imidazole	942.8	64.0	240	183	13
Pyridine	930.0	85.7	46	47	8.8
Pyrazole	894.1	73.0	21	17	9.3
Benzoxazol	891.6	38.0	[d]	[d]	0.75
DMSO	884.4	—	101	85	[e]
Isoxazole	848.6	47.0	[d]	[d]	[e]
4-Hydroxy-naphthalimide—					
Imidazole	942.8	64.0	900	615	9.6
Pyridine	930.0	85.7	138	137	8.9
Pyrazole	894.1	73.0	44	26	7.6
Benzoxazol	891.6	38.0	[d]	[d]	1.8
DMSO	884.4		191	195	[e]
Isoxazole	848.6	47.0	[d]	[d]	[e]

[a] From absorption spectra. [b] From fluorescence spectra. [c] From fluorescence lifetime measurements. [d] No hydrogen-bonding can be detected. [e] No quenching.

steady-state fluorescence intensities in the absence (I_0) and the presence of pyridine (I) shows an upward curvature (Fig. 4). This suggests that the fluorophore can be quenched both in dynamic and static processes. If the static quenching is attributed entirely to ground state hydrogen-bonding, the modified form of the Stern–Volmer equation describes the variation of I_0/I *vs.* quencher concentration.[27]

$$I_0/I = (1 + K[\text{quencher}])(1 + k_q \tau_0[\text{quencher}]) \quad (7)$$

where τ_0 refers to the lifetime of singlet excited hydroxy-naphthalimide, k_q is the rate constant of the dynamic quenching and K denotes the equilibrium constant of complex formation in the ground state. The quenching rate constants (k_q) were determined by time-resolved fluorescence technique (*vide infra*) and the K values were calculated by the nonlinear least-square fit of eqn. (7) to the experimental data. It is apparent in Fig. 4 that the calculated curves describe very well the experimental results. Table 2 demonstrates that the hydrogen-bonding equilibrium constants derived from both absorption and fluorescence measurements closely agree.

Addition of pyridine to the solutions of hydroxy-naphthalimides shortens the lifetime of the lowest singlet excited state. The fluorescence decays are well described by a single exponential function. The fluorescence lifetimes in the absence (τ_0) and the presence (τ) of pyridine are plotted in Fig. 4 based on the following equation:

$$\tau_0/\tau = 1 + k_q \tau_0[\text{quencher}] \quad (8)$$

Since the fluorescence decay times are influenced only by dynamic quenching, linear correlation is found between τ_0/τ and the quencher concentration. The quenching rate constants (k_q) derived from the slopes are given in the last column of Table 2.

Benzoxazole and isoxazole. In order to reveal the major factors controlling the rate of the hydrogen-bonding induced fluorescence quenching, we extended our studies to heterocyclic compounds containing a five-membered ring. Isoxazole affects neither the fluorescence decay nor the spectral characteristics of hydroxy-naphthalimides indicating that no interaction occurs between these compounds either in the ground or the excited state. However, the effect of benzoxazole resembles that observed for pyridine. Time-resolved fluorescence measurements proved that dynamic quenching takes place but the reaction rate is much lower than that of pyridine. No clear indication was found for ground state hydrogen-bonding because of the overlap between the benzoxazole and the hydroxy-naphthalimide absorption.

Pyrazole and imidazole. Compounds containing two heterocyclic nitrogens in a five-membered ring induce a different type of fluorescent behavior. They not only quench the fluorescence of hydroxy-naphthalimides but also cause a new fluorescence in the 500–800 nm spectral range whose intensity increases with the quencher concentration. It is apparent in Fig. 5 that the new emission consists of two bands for 3-HONI + imidazole and 3-HONI + *N*-methylimidazole solutions, whereas in the other cases no such clear evidence can be observed for dual luminescence in the long wavelength band.

The short wavelength (SW) emission around 370–480 nm originates from the excited hydroxy-naphthalimides. The fluorescence lifetimes measured in this band decrease with increasing concentration of pyrazole and imidazole. This proves that dynamic quenching occurs. Fig. 6 gives the Stern–Volmer plots of the data obtained by steady-state and time-resolved fluorescence techniques for HONI–imidazole systems. In contrast with the linear dependence obtained from lifetime measurements, the Stern–Volmer plots of the steady-state fluorescence intensities are concave indicating that static quenching has an important contribution as well. The red-shifts and the isosbestic points in the absorption spectra suggest 1 : 1 hydrogen-bonding. The experimental data were analyzed as described above for the other additives and the results are included in Table 2.

The most interesting feature of the spectra in Fig. 5 is the appearance of the long-wavelength (LW) emissions, which are attributed to the singlet excited complexes of hydroxy-naphthalimide with pyrazole and imidazole. The extent of proton transfer within these complexes is probably very sensitive to the acid–base properties of the constituents and the local polarity of the solvate shell.

In the case of 3-HONI, the SW and the LW bands are well-separated, therefore, we could readily see the formation and the decay of the species emitting in these spectral ranges. The variation of the fluorescence intensity as the function of time is presented in Fig. 7 for the solution containing 3-HONI and 0.024 M imidazole. The dotted line in Fig. 7A exhibits the fluorescence decays detected at 405 and 640 nm, whereas the continuous lines represent the fitted curves (*vide infra*), which were calculated by a non-linear least-squares deconvolution method. The parameter describing the rise of the signal at 640 nm (1.3 ns) perfectly agrees with the decay parameter obtained at 405 nm. The excitation pulse profile (dotted line) and the growing in of the fluorescence at 640 nm are shown in Fig. 7B using a better time resolution. The calculated curves match the measured data so well that they are hardly distinguishable in the figure. The fluorescence decay at 405 nm can be well described with a single exponential function. (The signal shown in Fig. 7A has 1.3 ns lifetime.) The time-resolved fluorescence of the 3-HONI–imidazole complex exhibits more complex kinetics. The data were analyzed with a double exponential function:

$$C_2 \exp(-t/\tau_2) - C_1 \exp(-t/\tau_1) \quad (9)$$

where t denotes time, C_1 and C_2 are constants. Calculation resulted in $\tau_1 = 1.3$ ns and $\tau_2 = 4.9$ ns for the decay constants when 0.024 M imidazole concentration was used. The C_1/C_2 ratio is expected to be 1 if the species emitting at long wavelengths is produced only in the quenching reaction.[28] We found $C_2/C_1 = 1.57$, which clearly indicates that both the direct excitation of the ground state hydrogen-bonded complex and the dynamic quenching of the singlet excited 3-HONI result in LW emission. As it is expected for a pseudo-first-order process, the growing in of the LW fluorescence and the decay of the SW fluorescence strongly depend on the concentration of the quencher. However, the decay time of the LW emission only slightly decreases with the quencher concentration.

It is evident from the spectra displayed in Fig. 5 that the excited hydrogen-bonded complexes of pyrazole have different characteristics compared with that of imidazole and *N*-methylimidazole. In the former case, the LW emissions have a Gaussian shape with maxima at 600 nm and 520 nm for 3-HONI and 4-HONI, respectively. Since these maxima are at higher energies than the fluorescence peak of the deprotonated hydroxy-naphthalimides (Fig. 2), we suggest that only a partial proton shift takes place along the hydrogen-bond in these excited complexes.

It is especially noteworthy that the addition of imidazole to the 3-HONI solution leads to structured LW fluorescence, which can be resolved to two components (Fig. 5A). In order to exclude the possibility that one of the LW fluorescence components originates from the interaction of 3-HONI with imidazole dimer[29] we studied the reactions of *N*-methylimidazole as well. This compound is not able to form a hydrogen-bonded dimer because it does not contain an N–H moiety. Fig. 5A demonstrates that the structured LW emission appearing in the presence of *N*-methylimidazole resembles that obtained with imidazole. Thus, we can rule out that

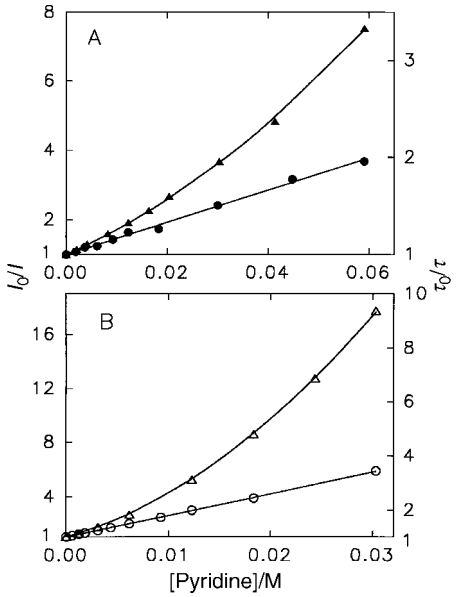

Fig. 4 Stern–Volmer plots of the results obtained by time-resolved and steady-state fluorescence technique for HONI–pyridine systems in CH_2Cl_2. (A) 3-HONI: ▲, steady-state measurements, ●, time-resolved measurements. (B) 4-HONI: △, steady-state measurements, ○, time-resolved measurements.

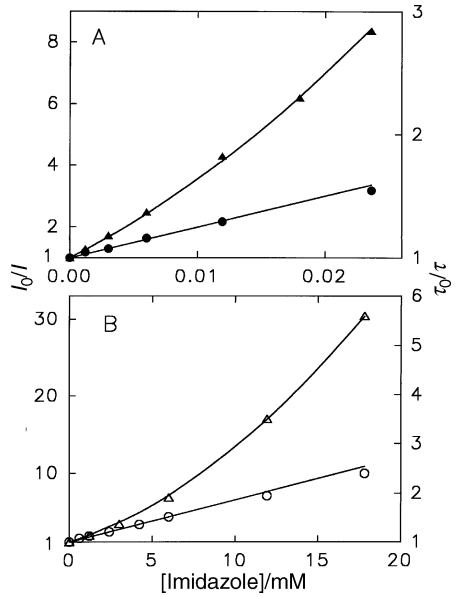

Fig. 6 Stern–Volmer plots of the data obtained by steady-state and time-resolved fluorescence techniques for the HONI—imidazole systems in CH_2Cl_2. (A) 3-HONI: ▲, steady-state measurements; ●, time-resolved measurements. (B) 4-HONI: △, steady-state measurements; ○, time-resolved measurements.

dimerization of the additive causes the dual emission at long wavelengths.

The relative intensity of the two fluorescence bands in the 500–800 nm spectral domain is temperature dependent both in ethyl acetate and in CH_2Cl_2. The substantial increase of the higher energy component is particularly discernible in the 295–181 K temperature range in ethyl acetate where the two bands are better separated than in CH_2Cl_2.

It is readily seen in Fig. 8 that the intensity ratio of the two emissions in the 500–800 nm region strongly depends on the media. In acetonitrile, the band with a maximum around 550 nm disappears, and, likewise, addition of ethanol in the CH_2Cl_2 solution significantly weakens this emission. Our results indicate that in solvents of medium polarity the 3-HONI–imidazole excited complexes have two dominant structures which differ in the extent of their proton shift. However, the complex that fluoresces at higher energies is bound with a hydrogen-bond and possesses only a limited proton transfer character when the proton is removed from the HO group toward the heterocyclic nitrogen in the species emitting at long wavelengths. The identical fluorescence decay times throughout the LW bands of the 3-HONI–imidazole complex in CH_2Cl_2 suggest that a fast equilibrium is established between the two types of complex. The polar solvents weaken the hydrogen-bond and promote proton transfer, therefore, no dual emission can be seen in acetonitrile. The ion-pair character of the complex in acetonitrile is supported by the fact that the fluorescence maximum of both the 3-HONI–imidazole complex (Fig. 8) and the 3-HONI anion (Fig. 2A) are located around 630 nm in this polar solvent.

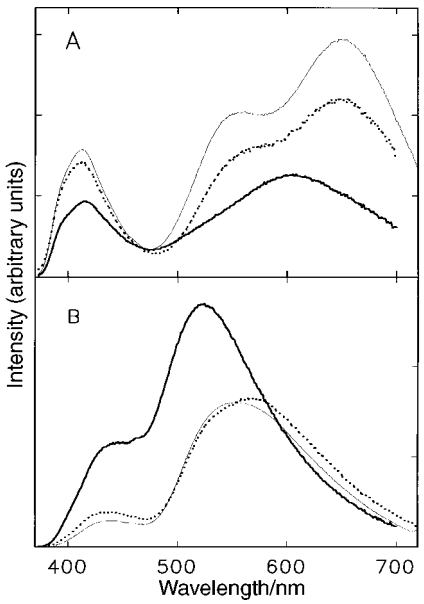

Fig. 5 Fluorescence spectra in CH_2Cl_2. (A) 3-HONI in the presence of 0.156 M pyrazole (heavy line), 0.024 M imidazole (dotted line) and 0.024 M *N*-methylimidazole (thin line); (B) 4-HONI in the presence of 0.057 M pyrazole (heavy line), 0.018 M imidazole (dotted line) and 0.018 M *N*-methylimidazole (thin line).

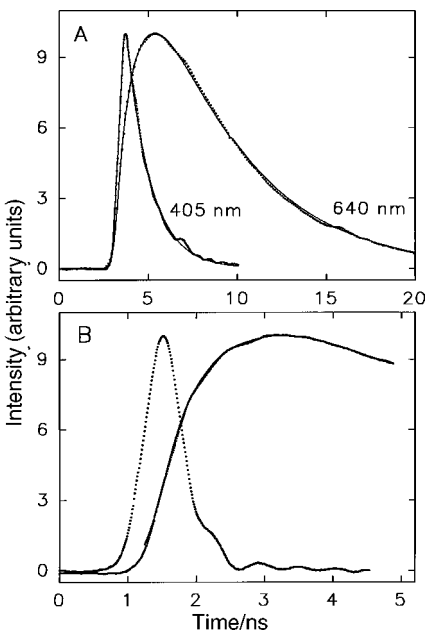

Fig. 7 Fluorescence decays in 3-HONI + 0.024 M imidazole solution in CH_2Cl_2. (A) Fluorescence decay (dotted line) and fitted curve (continuous line) at 405 nm and 640 nm. (B) Excitation pulse profile (dotted line), fluorescence growing in and fitted curve (continuous line) at 640 nm.

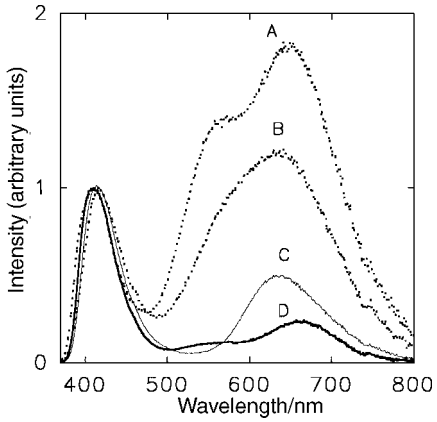

Fig. 8 Fluorescence spectra of 3-HONI in the presence of 0.024 M imidazole: (A) in CH_2Cl_2, (B) in CH_2Cl_2 + 0.17 M EtOH, (C) in the presence of 0.052 M imidazole in acetonitrile and (D) in ethyl acetate.

Comparison of the effects of the various hydrogen-bond acceptors. It was demonstrated that the intermolecular hydrogen-bonding with alcohols in the singlet excited state acts as an effective accepting mode of radiationless deactivation for aromatic carbonyl compounds.[2–6] We should comment on the question of why hydroxy-naphthalimides, which also contain carbonyl groups, are not quenched by the strong hydrogen-bond donor TFE. For the example of 2-substituted fluorenones we demonstrated that efficient hydrogen-bonding induced internal conversion can occur only if the carbonyl oxygen has high electron density in the excited state.[30] As stated above, the absorption and the fluorescence spectra of hydroxy-naphthalimides exhibit small solvatochromic shifts because excitation leads to minor change in the dipole moment. Theoretical calculations also corroborated that there is no significant difference in the electron density of the carbonyl oxygen for the S_0 and the S_1 states of naphthalimides,[12,31] therefore, hydrogen-bonding with TFE does not accelerate the internal conversion process.

Table 2 lists the hydrogen-bonding equilibrium constants and the quenching rate constants obtained by different methods. The proton affinities[32] and the Bird aromaticity indices[33] for the quenchers are also included. Katritzky *et al.* showed that the Bird aromaticity index is the best measure of the classical aromaticity,[34] therefore, we chose this among the various aromaticity parameters available in the literature. The rate constant of the excited hydroxy-naphthalimide quenching varies remarkably with the molecular structure of the hydrogen-bond acceptor; no quenching takes place with isoxazole but the reaction is diffusion controlled in the case of imidazole. A parallel change can be seen between the proton affinity and the k_q rate constants throughout the series of the quenchers shown in Table 2. The reactants that have low proton affinity do not promote the deactivation of the singlet excited hydroxy-naphthalimides. The hydrogen-bonding power of the additives, as measured directly by the ground state hydrogen-bonding equilibrium constants (K), does not play a rate determining role because no correlation can be found between the K and k_q quantities. For example, DMSO does not quench the fluorescence of hydroxy-naphthalimides in spite of the fairly large hydrogen-bonding equilibrium constant in the ground state. These results suggest that proton displacement plays a crucial role in the interaction of excited hydroxy-naphthalimides and hydrogen-bond acceptors.

It is not surprising that no correlation appears between the ground state hydrogen-bonding equilibrium constants and the proton affinities listed in Table 2. Gurka and Taft established that hydrogen-bonding and basicity are unrelated.[35] For example, using a common hydrogen-bond donor, they showed that the pK_a of a carbonyl compound is 13 powers of ten less than that of the corresponding amine for equal values of hydrogen-bonding equilibrium constant.[36] Moreover, the data reported by Abraham *et al.* demonstrate that DMSO forms stronger hydrogen-bonds than the much more basic pyridine derivatives.[37]

Coupled electron–proton movement was suggested to promote the radiationless deactivation when a heterocyclic molecule containing an aromatic π-electronic system is connected to excited hydroxyarenes directly *via* a hydrogen-bond.[10] The extremely weak fluorescence for the hydrogen-bonded complexes of benzoxazole and pyridine with hydroxy-naphthalimides is probably due to a rapid internal conversion *via* a similar process. The proton shift toward the hydrogen-bond acceptor induces efficient nonradiative energy dissipation. However, the intensive emission as well as the long lifetime (*ca.* 4–9 ns) of the excited hydrogen-bonded complexes containing imidazole and pyrazole obviously indicate slow internal conversion (k_{IC} value of *ca.* 10^8 s^{-1} can be deduced from the experimental data). We did not find a correlation between the aromaticity index of the hydrogen-bond acceptor and the radiationless deactivation rate of the excited hydrogen-bonded complex. This seems to indicate that the energy dissipation mechanism suggested for the excited hydroxyarene–pyridine species does not play a dominant role if other types of nitrogen heterocyclics serve as the hydrogen-bond acceptor.

Acknowledgements

We very much appreciate the support of this work by the Hungarian Science Foundation (OTKA, Grant T 023428) and the scientific exchange program between the French Ministry of Foreign Affairs and the Hungarian Committee for Technological Development (Balaton Project F-10/97).

References

1 J. Herbich, C.-Y. Hung, R. P. Thummel and J. Waluk, *J. Am. Chem. Soc.*, 1996, **118**, 3508 and references therein.
2 H. Inoue, M. Hida, N. Nakashima and K. Yoshihara, *J. Phys. Chem.*, 1982, **86**, 3184.
3 R. S. Moog, N. A. Burozski, M. M. Desai, W. R. Good, C. D. Silvers, P. A. Thompson and J. D. Simon, *J. Phys. Chem.*, 1991, **95**, 8466; J. Ritter, H. U. Borst, T. Lindner, M. Hauser, S. Brosig, K. Bredereck, U. E. Steiner, D. Kühn, J. Kelemen and H. E. A. Kramer, *J. Photochem. Photobiol. A*, 1988, **41**, 227; H. U. Borst, J. Kelemen, J. Fabian, M. Nepras and H. E. A. Kramer, *J. Photochem. Photobiol. A*, 1992, **69**, 97.
4 L. Biczók, T. Bérces and H. Linschitz, *J. Am. Chem. Soc.*, 1997, **119**, 11071.
5 T. Yatsuhashi and H. Inoue, *J. Phys. Chem. A*, 1997, **101**, 8166.
6 T. Yatsuhashi, Y. Nakajima, T. Shimada, H. Tachibana and H. Inoue, *J. Phys. Chem. A*, 1998, **102**, 8657.
7 C. Turró, C. K. Chang, G. E. Leroi, R. I. Cukier and D. G. Nocera, *J. Am. Chem. Soc.*, 1992, **114**, 4013.
8 R. I. Cukier and D. G. Nocera, *Annu. Rev. Phys. Chem.*, 1998, **49**, 337.
9 W. J. Liegh, E. C. Lathioor and M. J. St Pierre, *J. Am. Chem. Soc.*, 1996, **118**, 12339.
10 N. Mataga and H. Miyasaka, *Prog. React. Kinet.*, 1994, **19**, 317 and references therein.
11 H. Miyasaka, K. Wada, S. Ojima and N. Mataga, *Isr. J. Chem.*, 1993, **33**, 183.
12 V. Wintgens, P. Valat, J. Kossanyi, A. Demeter, L. Biczók and T. Bérces, *New J. Chem.*, 1996, **20**, 1149.
13 L. M. Tolbert and J. E. Haubrich, *J. Am. Chem. Soc.*, 1990, **112**, 8163.
14 L. M. Tolbert and J. E. Haubrich, *J. Am. Chem. Soc.*, 1994, **116**, 10593.
15 D. Huppert, L. M. Tolbert and S. Linares-Samaniego, *J. Phys. Chem. A*, 1997, **101**, 4602.
16 V. Wintgens, P. Valat, J. Kossanyi, L. Biczók, A. Demeter and T. Bérces, *J. Chem. Soc., Faraday Trans.*, 1994, **90**, 411.
17 W. Adam, X. Quian and C. R. Saha-Möller, *Tetrahedron*, 1993, **49**, 417.

18 R. Royer, J. P. Buisson, P. Demerseman and J. P. Lechartier, *Bull. Soc. Chim. Fr*., 1969, 2792.
19 W. M. Rodionow and A. M. Fedorowa, *Bull. Soc. Chim. Fr*., 1939, 479.
20 P. Valat, V. Wintgens, J. Kossanyi, L. Biczók, A. Demeter and T. Bérces, *J. Am. Chem. Soc*., 1992, **114**, 947.
21 S. L. Murov, G. L. Carmichael and I. Hug, *Handbook of Photochemistry*, Marcel Dekker, New York, 2nd edn., 1993.
22 J. K. Hurley, N. Sinai and H. Linschitz, *Photochem. Photobiol*., 1983, **38**, 9.
23 T. Förster, *Z. Electrochem*., 1950, **54**, 531.
24 The HyperChem program package was used. The geometry of the molecule was optimized by AM1 calculation and the energy levels were obtained by ZINDO/S method.
25 A. Prado, J. Campanario, J. M. L. Poyato, J. J. Camacho, D. Reyman, E. Martin, *THEOCHEM*., 1988, **166**, 463.
26 N. Mataga and S. Tsuno, *Bull. Chem. Soc. Jpn*., 1957, **30**, 368.
27 J. R. Lakowicz, *Principles of fluorescence spectroscopy*, Plenum Press, New York, 1983, p. 266.
28 D. V. O'Connor, L. Chewter and D. Phillips, *J. Phys. Chem*., 1982, **86**, 3400.
29 E. Fischer, *Ber. Bunsen-Ges. Phys. Chem*., 1969, **73**, 1007.
30 L. Biczók, T. Bérces and H. Inoue, *J. Phys. Chem. A*., 1999, **103**, 3837.
31 M. Adachi, Y. Murata and S. Nakamura, *J. Phys. Chem*., 1995, **99**, 14240.
32 E. P. L. Hunter and S. G. Lias, *J. Phys. Chem., Ref. Data*, 1998, **27**, 707.
33 C. W. Bird, *Tetrahedron*, 1985, **41**, 1409; *ibid*., *Tetrahedron*, 1986, **42**, 89.
34 A. R. Katritzky, M. Karelson and N. Malhotra, *Heterocycles*, 1991, **32**, 127.
35 D. Gurka and R. W. Taft, *J. Am. Chem. Soc*., 1969, **91**, 4794.
36 R. W. Taft, D. Gurka, L. Joris, P. von R. Schleyer and J. W. Rakshys, *J. Am. Chem. Soc*., 1969, **91**, 4801.
37 M. H. Abraham, P. P. Duce, D. V. Prior, D. G. Barrett, J. J. Morris and P. J. Taylor, *J. Chem. Soc., Perkin Trans. 2*, 1989. 1355.

Paper 9/04520A